Biochimica et Biophysica Acta, 1059 (1991) 265–274

ADONIS 0005272891002016

BBABIO 43465

The behavior of a fast-responding barbituric acid potential-sensitive molecular probe in bovine heart submitochondrial particles

T.V. Tran, S. Allen and J.C. Smith

Department of Chemistry and Laboratory for Microbial and Biochemical Sciences, Georgia State University, Atlanta, GA (U.S.A.)

(Received 13 May 1991)

Key words: Molecular probe; Membrane potential; Energy transduction; (Mitochondria); (Membrane)

The barbituric acid probe diBa-C_2-(5) responds to the formation of a membrane potential ($\Delta\Psi$) in bovine heart submitochondrial particles (SMP) by a CCCP-reversible, 5–7 nm red shift of the probe absorption spectrum. This shift can be enhanced by the addition of nigericin, an observation that indicates that the probe is specifically sensitive to $\Delta\Psi$. Probe-SMP binding analyses indicate that, relative to the resting state, the ratio of the dye dissociation constant to the maximum number of binding sites decreases by a factor of 30 when $\Delta\Psi$ is generated. This observation suggests that the origin of the potential-dependent shift of the probe absorption spectrum is increased occupancy of the SMP membrane by diBa-C_2-(5). The time course of the ATP-induced diBa-C_2-(5) spectral shift in SMP was complete in nominally 0.2 s and could be described by a single-exponential rate equation. There was no evidence for a slower-phase signal when the data collection time period was increased to 250 s. The apparent first-order rate constants obtained from the single exponential analyses of the barbituric acid ATP-generated signal, however, were a linear function of probe concentration at fixed SMP membrane concentration. The resulting second-order rate constant obtained by linear regression was nominally $1 \cdot 10^7$ M(dye)$^{-1}$ s^{-1}; this value is two to three orders of magnitude higher than that of a number of other well-established probes of $\Delta\Psi$ in mitochondrial preparations. Based on the invariance of the kinetics of the oxidation of cytochromes *c* and c_1 by ATP-driven reversed electron transport in the presence and absence of the probe, diBa-C_2-(5) does not appear to permeate the SMP membrane on a time scale of milliseconds to several minutes.

Introduction

Molecular probes of the polyene class have proven to be useful indicators of electrical potential gradients in a variety of membrane preparations ranging from model bilayers and reconstituted preparations to tissue and organ level studies. The potential sensitivity of these probes is manifested in terms of changes in one or more parameters associated with the optical properties of these indicators. The application of the several classes of both extrinsic and intrinsic probes in diverse membrane preparations has been summarized in a number of reviews and monographs including those by Smith [1], Bashford [2], Bashford and Smith [3] and Waggoner [4,5]. A multi-volume series dealing with spectroscopic probes was edited by Loew [6]. Cohen and Salzberg [7] have dealt with the use of extrinsic probes primarily in physiological preparations. The application of potential-sensitive probes in cell biology has been described in a monograph edited by de Weer and Salzberg [8].

In addition to the detection and quantitation of membrane potential gradients, the elucidation of the elementary steps in the generation of potential gradients in energy-transducing membranes is one of the more attractive applications of these indicators. Studies based on the use of intrinsic carotenoids and extrinsic styryl-type charge shift probes in photosynthetic sys-

Abbreviations: ATP, adenosine 5′-triphosphate; CCCP, carbonylcyanide-m-chlorophenylhydrozone; $\Delta\Psi$, transmembrane electrical potential gradient; LCAO-SCF-CI, linear combination of atomic orbitals-self consistent field-configuration interaction; NADH, β-nicotinamideadenine dinucleotide, reduced form; QCPE, Quantum Chemistry Program Exchange.

Correspondence: J.C. Smith, Department of Chemistry and Laboratory for Microbial and Biochemical Sciences, Georgia State University, Atlanta, GA 30303, U.S.A.

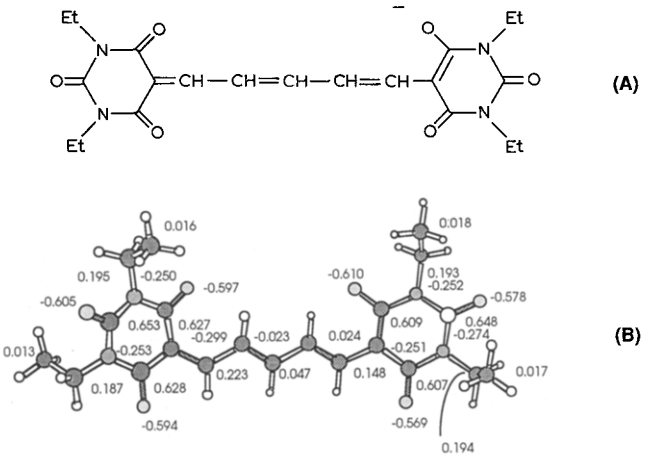

Fig. 1. (A) The structure of N^1,N^3-diethyl-5-[5'-[$N^{1''},N^{3''}$-diethyl-2,4,6-trioxo-1,2,3,4,5,6-hexahydropyrimidin-5''-ylidene]penta-1',3'-diene-1'-yl]barbituric acid (diBa-C_2-(5)); the probe exists in the deprotonated form at the medium pH used in the experiments described in this communication, since the pK of the hydroxyl group is approx. 4 (A.S. Waggoner, personal communication). (B) The diBa-C_2-(5) structure resulting from energy minimization with the default values of the AMBER force field using the MACROMODEL molecular mechanics package. The numbers near the atoms are the charges resulting from a LCAO-SCF-CI calculation using the AMPAC package. Additional energy minimization with the AMBER charges replaced by those from the AMPAC calculation resulted in virtually no additional structural changes. Details are provided in the Computational procedures section.

tems are well-known examples in this case [9–12]. Fast responding, charge shift or electrochromic, potential-dependent signals from carotenoids incorporated into the mitochondrial membrane or extrinsic styryl-type probes in mitochondrial preparations have, however, not yet been demonstrated, and the response time of the several available probes that function in mitochondrial preparations is probably too slow to allow insight into the elementary process(es) leading to the formation of transmembrane potential gradients ($\Delta\Psi$) to be obtained. In this communication are described the properties of a barbituric acid probe, diBa-C_2-(5), the spectral response of which to $\Delta\Psi$ in bovine heart submitochondrial particles (SMP) is significantly faster than that of a number of other well-established indicators. The barbituric acids have been employed in the detection and measurement of potential gradients in a number of intact cell preparations [2,6,8], but not extensively in submitochondrial particles. The structure of diBa-C_2-(5) is shown in Fig. 1.

Materials and Methods

ATP (from equine muscle), NADH (from yeast, grade III, disodium salt), succinate, nigericin, CCCP, bovine serum albumin and Hepes buffer were obtained from Sigma. All other reagents were purchased from Fisher Scientific and were of reagent grade or better. Stock solutions of diBa-C_2-(5) were prepared 0.5 mM in ethanol, protected from light by aluminum foil and stored in the dark at −20 °C. Stock solutions of CCCP and nigericin were also prepared in ethanol at a concentration of 1 mM and stored as previously described. Aliquots from the stock solutions were added directly to the aqueous buffer solution used in these investigations and described in the legend to Fig. 2.

Submitochondrial particles (SMP) were prepared from heavy bovine heart mitochondria according to the procedure of Thayer et al. [13] involving incubation of the mitochondria overnight in a substrate-containing medium prior to sonication for 35 s with a Heat Systems (Farmingdale, New York, U.S.A.) Model W-225R cell disrupter using a stainless steel container packed in ice followed by slow-speed centrifugation to remove mitochondrial debris and finally pelleting the SMP in a second centrifugation step. The SMP pellet was resuspended in 0.25 M sucrose and stored in small aliquots at −20 °C. The coupling of the resulting preparation was monitored in terms of the respiratory control ratio using a Rank Brothers (Bottisham, Cambridge, U.K.) oxygen electrode the output from which was fed to a Johnson Foundation amplifier and then to a Fisher 5000 series strip chart recorder. Typical respiratory control ratio values obtained using NADH as substrate and CCCP as an uncoupler to stimulate respiration were in the 4–5 range. Mitochondrial protein concentrations were obtained by means of the Biuret procedure; calibration plots were generated from solutions of bovine serum albumin in the same medium as that used for the SMP suspensions. The probe diBa-C_2-(5) was generously supplied by Professor A.S. Waggoner; it is not commercially available.

Optical spectroscopy

The absorption spectrum of diBa-C_2-(5) in SMP suspensions was obtained using a Johnson Foundation DBS-2 scanning double-beam spectrometer that operates on the dual-wavelength principle and, hence, virtually eliminates light scattering artifacts. Titrations needed for determining probe-membrane binding parameters were carried out a fixed wavelengths using the DBS-2 instrument.

Time-resolved investigations were carried out with either an Aminco-Morrow rapid mixing device, purchased from SLM Instrument Co., Urbana, IL, adapted to the DBS-2 spectrometer with data acquisition and analysis by an On Line Instruments 3820 system, Jefferson, GA, or with a High Tech Ltd. (Wiltshire, U.K.) SF-51 stopped-flow spectrometer system. In the latter system, data acquisition and analysis was accomplished with the HS-1 software package furnished by the manufacturer. The time resolution of the Aminco-Morrow/DBS-2 system is nominally 5 ms and that of the High Tech Ltd. SF-51 system is 1 ms. The choice of

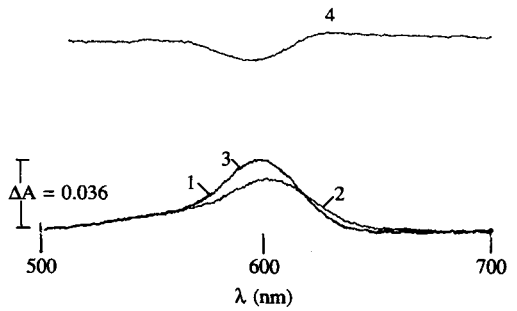

Fig. 2. The absorption spectrum of diBa-C_2-(5) in the presence of SMP, trace 1. The addition of ATP-$MgCl_2$ caused a shift in the spectrum and loss of absorbance especially near 600 nm, trace 2, that can be completely reversed by the uncoupler CCCP, trace 3. Trace 4 illustrates the enhancement of the ATP-dependent spectral shift caused by nigericin and indicates that diBa-C_2-(5) is specifically sensitive to $\Delta\Psi$ in SMP; seen the Discussion section for details. Medium: 0.25 M sucrose, approximately 50 μM KCl, and 10 mM Na-Hepes (pH 7.5). Concentrations: 2.05 μM diBa-C_2-(5), 0.29 mg/ml SMP protein, 5 μM CCCP, 2.5 mM ATP-$MgCl_2$, 0.1 μM nigericin. Temperature: 21° C. Reference wavelength: 550 nm. The absorbance calibration marker is common to all four traces shown in this figure.

610 nm at which to monitor the development of the ATP-generated probe signal corresponds to a wavelength near an extremum in the difference spectrum of the uncoupled and ATP-energized probe-SMP system; the extremum value, however, was a function of the probe-to-membrane concentration ratio; the 610 nm value is a compromise value suitable for the range of this ratio covered in the time-resolved investigations. Experimental conditions are described in the appropriate figure legends.

Results and data analyses

The passive association of diBa-C_2-(5) with SMP causes a fraction of a nanometer red shift of the free probe spectrum and, hence, this spectrum is not shown in Fig. 2. The absorption spectrum of the probe in the presence of SMP is shown as trace 1 in Fig. 2; depending on the probe-to-membrane protein concentration ratio and the quality of the SMP preparation, the addition of ATP-$MgCl_2$ causes a 5 to 7 nm red shift of the spectrum, trace 2, that can be completely reversed upon addition of the uncoupler CCCP, trace 3. The ATP-induced shift in the probe absorption spectrum illustrated in trace 2 is enhanced by the addition of nigericin from a stock solution prepared as described in the previous section (trace not shown). The difference between the probe spectrum in the presence of ATP-$MgCl_2$ and nigericin and trace 2 is shown in the inset labeled trace 4. The magnitude of the ATP-induced shift of the diBa-C_2-(5) absorption spectrum was a function of the probe-to-membrane protein concentration ratio. The optimum range for this ratio was 4 to nominally 7 nmol dye/mg protein. Below the former value, little ATP effect on the probe spectrum was observed and above the latter value, the spectral shift magnitude tended toward saturation and began to decline. Similar shifts of the diBa-C_2-(5) absorption spectra were also observed when NADH and succinate were used as substrates to generate $\Delta\Psi$.

Controls were carried out for possible alterations of the probe optical spectral properties caused by changes in the medium ionic strength, since $MgCl_2$ was added in conjunction with ATP to generate membrane potentials in the SMP preparations used in these investigations. The probe-to-SMP membrane protein concentration ratio employed was 6.8 nmol probe/mg protein, the optimum concentration ratio for generating potential-dependent probe spectral shifts. The absorption spectra of the probe, obtained by dual-wavelength spectroscopy as previously described, in the presence and absence of 2.5 mM $MgCl_2$ were superimposable. When the concentration of $MgCl_2$ was raised to 17 mM, the highest value employed in these investigations, the absorbance values at 550 and 590 nm, the wavelength pair employed in the probe-SMP binding studies, were within the noise level of the control spectrum obtained in the absence of $MgCl_2$. The change in the absorbance at 610 nm when $MgCl_2$ was present at 17 mM was only $1.3 \cdot 10^{-3}$ ΔA units, or 0.7% of the full-scale absorbance change shown in the kinetics trace shown in Fig. 4. Since the probe absorption spectrum was insensitive to the presence of $MgCl_2$, none of the control spectra have been included in Fig. 2.

Probe-SMP binding analyses

The ratio of the probe-membrane dissociation constant (K_D) to the maximum number of probe binding sites (n), K_D/n, was determined by titrating a fixed quantity of diBa-C_2-(5) with SMP in a medium containing ATP-$MgCl_2$ or the uncoupler CCCP. This analysis requires the evaluation of an enhancement factor, ϵ, due to the association of the probe with the membrane: $\epsilon = P_i/P_0$ where P_0, in this case, is the absorbance of the free probe and the P_i are the several absorbance values observed as SMP aliquots are added to the probe solution. With the assumption that an effectively single class of probe sites exists in the membrane, the data are expected to obey the relationship [14]

$$\epsilon - 1 = (\epsilon_b - 1) - \frac{K_D}{n}\frac{(\epsilon - 1)}{m} \quad (1)$$

where m is the SMP membrane protein concentration and ϵ_b is the limiting enhancement factor obtained by extrapolation of the data to infinite membrane concentration where all probe is bound. A plot of $\epsilon - 1$ vs. $(\epsilon - 1)/m$ is expected to be linear; the negative of the

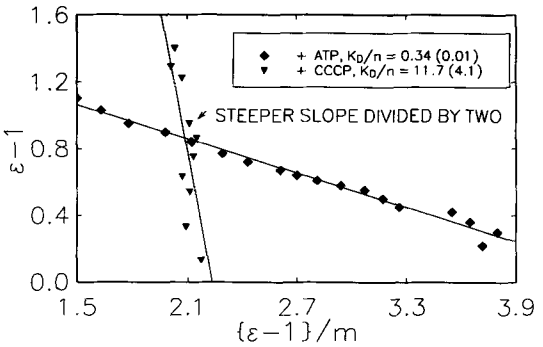

Fig. 3. Typical diBa-C_2-(5) binding data obtained from a titration of a fixed quantity of probe with SMP membrane. The enhancement factor $\epsilon = P_i/P_0$ where the parameter P_0 is the absorbance of the free probe at 550–590 nm and P_i are the values of the absorbance as a function of added SMP. The indicated wavelength pair was determined as the optimum choice based on the difference spectrum of the probe free and in the presence of SMP and was dictated in part by the weak binding of diBa-C_2-(5) to uncoupled SMP. The increment in the sample volume that results from the titration with aliquots from stock SMP suspensions has been taken into account in calculating the membrane concentration, m. The lines through the data points were obtained by linear regression analysis of these data. The medium is that given in the legend to Fig. 2. Initial concentrations: 10 μM diBa-C_2-(5), 10 μM CCCP, 17 mM ATP-$MgCl_2$. Temperature: 20 °C. The units of K_D/n are those of m, mg/ml membrane protein. The elevated value of the ATP-$MgCl_2$ concentration was used to ensure that the membrane potential was maintained by the SMP over the lengthy titration time periods that these experiments required.

slope of the linear regression line though the data is a measure of K_D/n. Typical diBa-C_2-(5)-SMP binding data are shown in Fig. 3 for ATP-energized SMP and those uncoupled by CCCP. The values of K_D/n for these two cases differ by a factor of nominally 30 with the value of K_D/n being the lower when ATP-$MgCl_2$ was present; values are provided in the inset in Fig. 3. The quantities in parentheses are standard errors in the ratios obtained from the slopes of the two plots. The error in K_D/n is significantly larger for uncoupled or unenergized SMP than that for the ATP-energized preparation, since the interaction of diBa-C_2-(5) with the unenergized membrane is weak; the spectral shift of the probe absorption spectrum caused by passive association of the probe with unenergized SMP is a fraction of a nanometer. The t distribution has been used to obtain a confidence interval such that the true slope, B, lies within this interval at a defined probability. The relevant equation [15] is:

$$B = b \pm t_\alpha \frac{S_{yx}}{\sqrt{\sum_{i=1}^{n} X_i^2 - n\bar{X}}} \qquad (2)$$

where b is the slope from the linear regression analysis of the plot of $\epsilon - 1$ vs. $(\epsilon - 1)/m$ (the X_i in Eqn. 2). $\bar{X}$ is the mean value of $(\epsilon - 1)/m$ and S_{yx} is the standard error of the estimate of y $(\epsilon - 1)$ on x; t_α is the area under the t distribution function for a given probability obtained by integrating the function over $\pm\alpha$. The confidence intervals of K_D/n for ATP-energized (0.341 ($\pm$0.026)) and uncoupled SMP (11.70 ($\pm$11.30)) do not overlap at a 0.97 probability or 3% significance level.

Time-resolved investigations

The time course of the ATP-induced diBa-C_2-(5) spectral shift (trace 2 of Fig. 2) was monitored by the substrate pulse technique [16]. In this procedure, the passive probe–SMP interaction is allowed to reach equilibrium in one of the syringes prior to mixing the

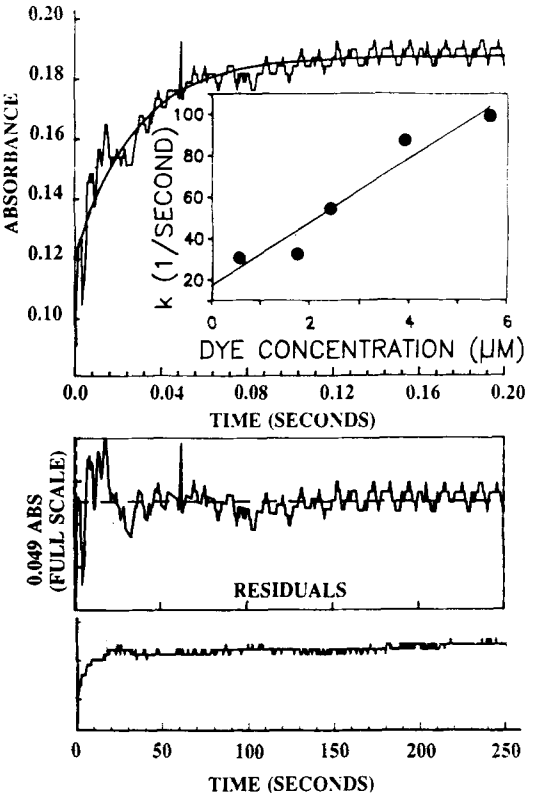

Fig. 4. The top trace is the time course of the ATP-induced diBa-C_2-(5) signal development in SMP suspended in the medium given in Fig. 2 at 20 °C and monitored at 610 nm. The noisier line is experimental data, and the smooth line is derived from a fit of the data to a single exponential rate equation. The apparent first-order rate constant obtained was 40 s^{-1}. Concentrations: 2 μM diBa-C_2-(5), 0.3 mg/ml membrane protein, and 6 mM ATP-$MgCl_2$. The RC time constant of the detector was set to 330 μs. The inset shown beneath the topmost probe kinetics trace contains a plot of the pseudo-first-order rate constants vs. probe concentration at fixed SMP concentration. Analysis of these data gives a second-order rate constant of $1.53(\pm 0.24)\cdot 10^7$ M^{-1} s^{-1}; the quantity in parentheses is the standard error in the slope obtained by linear regression. The coefficient of determination, r^2, for the plot was 0.93. The middle trace is a plot of the residuals resulting from the fit of the data to a single exponential rate equation. The lower trace is the time course of the ATP-induced diBa-C_2-(5) signal in SMP over a 250 s time span; no slower phase signal is present over this span. Experimental conditions were the same as described above.

contents of this syringe with ATP-$MgCl_2$ from the second syringe of the rapid mixing devices employed in these investigations. The absorbance change resulting from the ATP-induced probe spectral shift was complete in less than 0.2 s; see the top trace in Fig. 4. The time course of these data could be satisactorily described by a single-exponential rate equation. No slower phase signal was observed in rapid mixing experiments in which the data collection was extended to 250 s; see the bottom trace in Fig. 4. The apparent first-order rate constants extracted from the exponential fits of the data were, however, found to be a function of diBa-C_2-(5) concentration at fixed SMP protein concentration. Under conditions in which the probe was the reactant in excess, a plot of the rate constants vs. probe concentration was linear as shown in the inset in Fig. 4. The second-order rate constant obtained from this plot by linear regression analysis was nominally $1 \cdot 10^7$ M^{-1} s^{-1}. Details are provided in the legend to this figure.

For the purpose of monitoring reversed electron transport, an aliquot from a stock SMP preparation was added to 2 ml of the buffer described in the legend to Fig. 2. Normal electron transport stimulated by succinate was blocked by the addition of cyanide. The inhibited SMP suspension was divided into two 1-ml portions; one was used as a control and to the second was added the diBa-C_2-(5) probe from a 620 μM stock solution in ethanol yielding the probe-to-SMP membrane protein ratios given in Table I. The resulting 1-ml vol. containing either the control SMP sample or this sample plus the diBa-C_2-(5) was placed in one of the syringes of the High Tech Ltd. SF 51 stopped-flow apparatus. ATP-$MgCl_2$ prepared in the same buffer as the SMP samples was placed in the second syringe and reversed electron transport was initiated by mixing the SMP sample and the ATP. The sample absorbance was monitored at 540 nm, a wavelength that corresponds primarily to the oxidation of cytochromes c and c_1 [17,18]; although diBa-C_2-(5) absorbs at this wavelength, there was no detectable ATP-dependent probe absorbance change at 540 nm as illustrated in Fig. 2.

The time course of the 540 nm ATP-generated absorbance signal was multiphasic and contained a slower-phase component that developed over a period of several minutes. The data collected over a 400-s time period, the maximum collection time allowed by the High Tech Ltd. SF 51 software, required a double-exponential rate equation, of the form shown in Eqn. 3, for an adequate description as illustrated in Fig. 5A and B.

$$\sum_{i=1}^{2} (A_i[1-\exp(k_i t)]) + C \tag{3}$$

The A_i and k_i are, respectively, the amplitude or absorbance factors and the rate constants for the two terms in Eqn. 3; C is a baseline offset parameter. When the data collection time was substantially decreased, however, a much faster phase signal was also detected. This signal was monitored with a 0.2-s collection time, the same as that used for monitoring the probe ATP-dependent spectral shift signal illustrated in Fig. 4. The faster phase signal shown in Fig. 5C is virtually undetected when data is collected as described in Fig. 5A because only one data point per second is collected in the latter measurements. Due to the presence of a portion of the initial phase of the signal monitored in experiments with a 400 s collection time, a double-exponential rate equation of the form shown in Eqn. 3 was also required to describe the resulting data provided in Fig. 5C and D. The slower phase rate constants resulting from the latter analyses, however, were not accurately obtainable from the data

TABLE I

ATP-driven reversed electron transport kinetics in bovine heart submitochondrial particles in the presence of the probe diBa-C_2-(5)

The absorbance at 540 nm, primarily due to the oxidation of cytochromes c and c_1, was monitored as a function of time in these experiments which were performed at 20 °C. The High Tech Ltd. SF 51 stopped-flow apparatus was used to collect 400 data points in all measurements. Membrane protein concentration: 0.4 mg/ml. The figures given in parentheses are standard deviations. The rate constants given in this table were obtained from averages of data obtained from six to eleven experiments with the stopped flow apparatus.

k_1 (s^{-1})	k_2 (s^{-1})	Collection time (s)	Probe-to-SMP membrane ratio (nmol probe/mg protein)
117 (±15)	–	0.2	control, no probe
111 (±7)	–	0.2	6.8
0.071 (±0.002)	0.0082 (±0.0004)	400	control, no probe
0.071 (±0.001)	0.0083 (±0.0001)	400	6.8
119 (±6)	–	0.2	control, no probe
120 (±16)	–	0.2	31
0.076 (±0.006)	0.008 (±0.001)	400	control, no probe
0.074 (±0.006)	0.0082 (±0.0008)	400	31

collected over such a short (0.2 s) time scale and are not reported in Table I; the faster phase rate constants, however, are given in this table. The preceding series of observations were reproducible in replicate experiments based on different stock SMP samples. A comparison of the rate constants obtained from analyses of the data in panel A with the control in (B) and a comparison of the results given in panel C with the control in D indicate no differences in these parameters; values are provided in the figure legend. The procedures used in analyzing the reversed electron transport signal time course yielded nominally 10 percent precision for the several rate constants. Within the quoted precision, the presence of the probe diBa-C_2-(5) had no effect on any of these rate constants at a probe-to-SMP membrane protein ratio of either 6.8 or 31 nmol probe/mg protein; see Table I. The former ratio is in the same range as that in which the probe ATP-generated spectral shift was optimal (Fig. 2), and the latter ratio corresponds to a considerable increase, but still did not cause a reduction in the kinetics of the reversed electron transport process as expected for an electrophoretically driven probe permeation of the SMP membrane considered in the Discussion.

It should be noted that the faster phase signal shown in Fig. 5C is unlikely to be due to the diBa-C_2-(5) probe itself for three reasons: (i) there is no detectable ATP-generated probe absorbance change at 540 nm

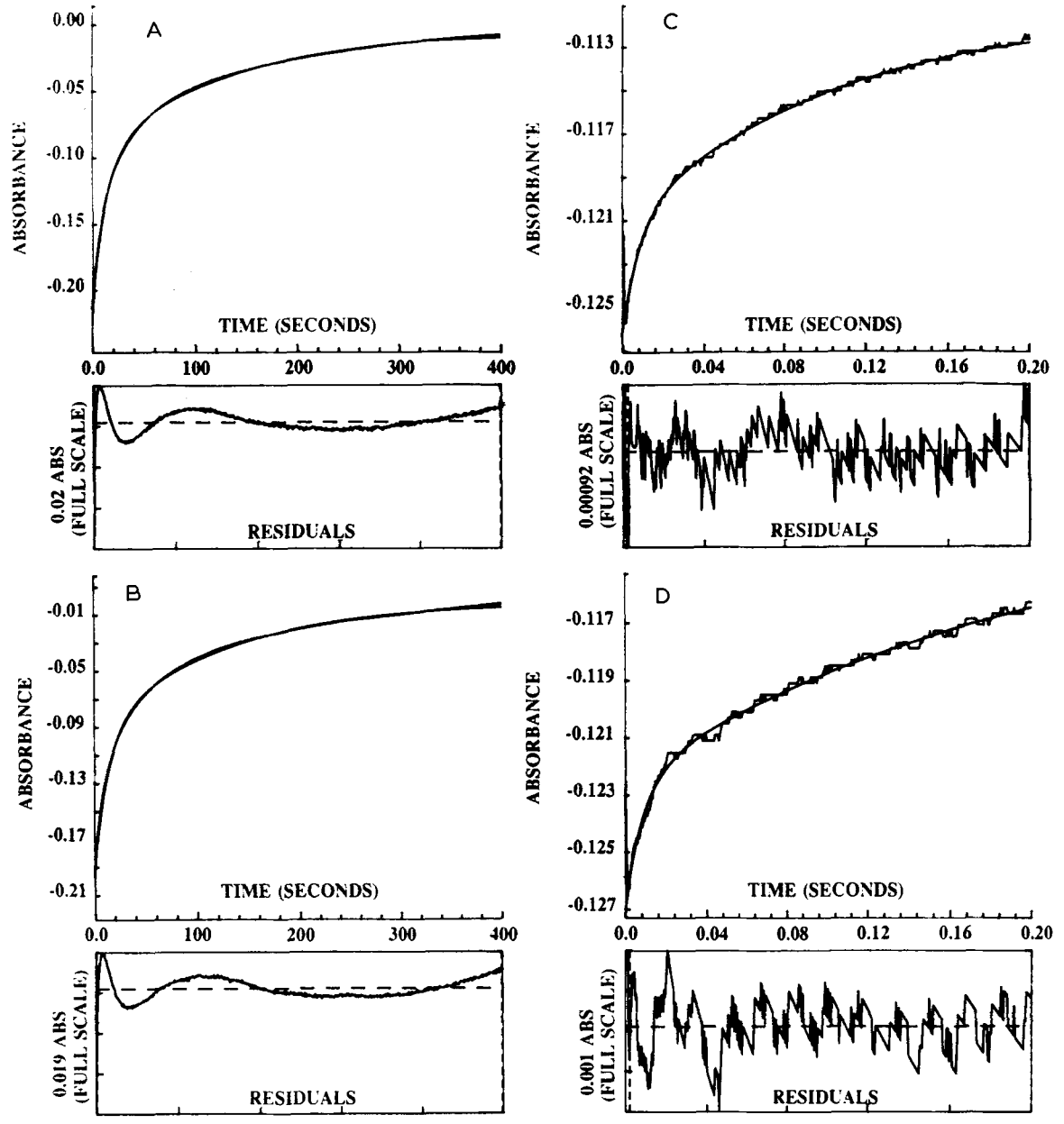

(Fig. 2), (ii) the observed rate constants provided in Table I did not change as the probe concentration was increased as would be expected if the faster phase signal contained a component from diBa-C_2-(5) based on the concentration dependence of the probe rate constants illustrated in Fig. 4, and (iii) the faster phase signal also developed in control, probe-free samples and was characterized by essentially the same rate constant as that resulting from the use of probe-containing samples.

Computational procedures

The diBa-C_2-(5) structure was generated on an Evans and Sutherland Model 390 molecular graphics system using the input mode of the molecular mechanics and dynamics package MACROMODEL and subjected to energy minimization by means of the default parameters in the AMBER force field. The atomic coordinates from the resulting probe structure were then used in the SCF-LCAO-CI package AMPAC (QCPE program No. 523). The MINDO/3 Hamiltonian was used in these calculations. For the case in which the probe geometry was fixed at that predicted by the energy minimization procedure of MACROMODEL, the resulting atomic charges are provided on the diBa-C_2-(5) structure shown in Fig. 1B, with the exception of probe hydrogen atoms. An additional energy minimization with MACROMODEL over 500 iterations using the AMBER force field, but with the AMBER atomic charges replaced by those returned by the AMPAC calculation reduced the energy of the probe by only 0.1 percent; the resulting structural changes were confined virtually exclusively to the ethyl groups. When the geometry of the probe was allowed to be optimized by AMPAC, unrealistic nonplanarity of the rings was predicted; the dihedral angles defined, for example, by the atoms with charges (Fig. 1B) 0.627 (C), −0.299 (C), 0.628 (C) and −0.253 (N), left ring and that by atoms with charges 0.609 (C), −0.251 (C), 0.607 (C) and −0.274 (N), right ring, increased from −1° and −1° in the structure shown in Fig. 1B to −26° and +28°, respectively, in the AMPAC geometry-optimized structure. The atomic charges on the geometry-optimized structure are similar to those resulting from the calculations on the probe with fixed geometry as given in Fig. 1B; the mean of the absolute value of the difference in atomic charges associated with the two structures was 0.025 (±0.019 S.D.) electronic charge units. The electronic energy of the geometry-optimized probe structure was within 1.5% of that of the initial diBa-C_2-(5) structure shown in Fig. 1B. Due to the distortion in the ring systems of diBa-C_2-(5), however, the geometry-optimized structure has not been employed in the analyses of the probe kinetics presented in a subsequent section. All calculations were performed on a Digital Equipment Corp. Microvax II or a Vaxstation 3100.

Discussion

The interaction of diBa-C_2-(5) with resting or uncoupled SMP is weak as judged by the very small shift

Fig. 5. The time course of the reversed electron transport signal in SMP monitored via the sample absorbance at 540 nm, a wavelength that correpsonds primarily to the oxidation of cytochromes *c* and c_1 [17,18]. The data presented in all parts of this figure were collected from SMP suspended at 0.4 mg/ml protein in the medium described in the legend to Fig. 2 and supplemented with 155 μM succinate and 77 μM KCN. The data shown in panels A and C were collected in the presence of diBa-C_2-(5) at a 31 nmol probe/mg protein concentration ratio, the higher value of this ratio employed in these investigations. The ATP-$MgCl_2$ concentration prior to the mixing of the contents of the two syringes was 9.8 mM. Temperature: 20 °C. Eqn. 3 in the text was required to fit the data over both the 400 and 0.2 s collection periods. The plots shown beneath the signal time course traces contain the residuals resulting from the analyses based on the previously described rate equation. The detector RC time constant was set to 330 μs; 400 data points were collected in all measurements. The transmission was adjusted to 100% prior to each data acquisition run. (A) A typical ATP-driven reversed electron transport signal from SMP in the presence of diBa-C_2-(5) monitored over a 400-s time span. The theoretical trace resulting from the fit of the data to the previously described rate equation and the experimental trace are virtually superimposed. The quality of the analysis in this case was not limited by the signal-to-noise ratio, but by the stability of the High Tech Ltd. instrument; an occasional drift in the signal over the lengthy collection time tended to cause small systematic deviations of the data from the theoretical trace. The rate constants and corresponding amplitudes obtained from this analysis are: $k_1 = 0.0743\ s^{-1}$; $A_1 = 0.112$ absorbance units; $k_2 = 0.00809\ s^{-1}$, $A_2 = 0.0966$ absorbance units. The amplitudes of the slower and faster phases were consistently found to be approximately equal. (B) The reversed electron transport signal from the SMP preparation without diBa-C_2-(5) present. The rate constants and amplitudes obtained from these data are: $k_1 = 0.0738\ s^{-1}$, $A_1 = 0.0931$ absorbance units; $k_2 = 0.00817\ s^{-1}$, $A_2 = 0.0931$ absorbance units. (C) A typical ATP-driven reversed electron transport signal from SMP in the presence of diBa-C_2-(5) monitored over a 0.2 s data collection time. The data points corresponding to the initial signal deflection toward larger negative absorbance were excluded from the analysis of the signal time course; excluded data are to the left of the dashed vertical line shown near zero time in the residuals plot. The noisier line is the experimental data, and the smooth trace is derived from fitting the data to Eqn. 3 in the text. The faster phase rate constant and amplitude obtained in this case are: $k_1 = 115\ s^{-1}$, $A_1 = 0.00536$ absorbance units. The slower phase parameters were not accurately obtainable from these data due to the short collection time. (D) The signal time course from SMP with no diBa-C_2-(5) present. The rate constants and amplitudes obtained form these data are: $k_1 = 113\ s^{-1}$, $A_1 = 0.00468$ absorbance units. As in panel C, excluded data are to the left of the dashed vertical line shown near zero time in the residuals plot. A summary of average rate constants obtained from these and similar analyses is given in Table I.

of the probe absorption spectrum observed under the preceding conditions and the relatively large value of K_D/n obtained from the analysis of the probe-SMP binding characteristics. This binding parameter ratio value is considerably larger than that characterizing the weak passive interaction of oxonol VI with SMP (0.49 mg/ml protein); see Ref. 16 and the inset in Fig. 3. The very nominal interaction of the probe with SMP in the absence of $\Delta\Psi$ is consistent with the weak hydrophobicity of the ethyl groups attached to the probe ring systems. The hydrophobicity of the aliphatic groups on probe ring systems has been found to correlate with the passive binding properties of a series of oxonol-type probes including oxonols V (R = phenyl), VI (R = *n*-propyl), VII (R = methyl), and VIII (R = *n*-nonyl) (our unpublished observations); the groups associated with R are substituents bonded to the isoxazole rings of these probes. The barbituric acid probe obtained by replacing the ethyl groups of diBa-C_2-(5) by *n*-butyl ones also binds to SMP much more strongly than does diBa-C_2-(5). The *n*-butyl derivative also has a tendency to bind to quartz cuvette walls and, hence, is unsuitable as a potential-sensing probe in SMP preparations. The generation of $\Delta\Psi$ by ATP addition, however, causes a substantial red shift of the diBa-C_2-(5) absorption spectrum. The behavior of the probe in this respect is similar to that of oxonol VI in SMP, although the 5–7 nm diBa-C_2-(5) spectral shift is not as large as the 15–20 nm shift observed in the case of oxonol VI under optimum conditions [16]. The enhancement of the ATP-induced diBa-C_2-(5) spectral shift by nigericin indicates that the probe is specifically sensitive to $\Delta\Psi$, since nigericin tends to diminish ΔpH, and $\Delta\Psi$ is increased proportionally to maintain a constant electrochemical gradient [19]. As described in the Results, the probe spectral properties were insensitive to changes in the medium ionic strength caused by the addition of $MgCl_2$ in conjunction with ATP; the potential-dependent spectral shift signal exhibited by diBa-C_2-(5) is, thus, unlikely to contain a significant surface potential component. Under the experimental conditions employed for these measurements, ATP hydrolysis generates a membrane potential of approx. 100 mV and a 135 mV contribution from the proton concentration gradient (ΔpH) [20]; since diBa-C_2-(5) is specifically sensitive to the membrane potential, the 5–7 nm spectral shift is thus generated by a $\Delta\Psi$ of nonimally 100 mV.

The diBa-C_2-(5)-SMP binding analysis suggests that the ATP-induced spectral shift is due to transfer of probe from the bulk aqueous phase and/or from the unstirred layer to membrane sites when $\Delta\Psi$ is generated. The binding data are consistent with a decrease in K_D, an increase in n or both such changes relative to the values of these parameters when no potential is present. The dependence of the ATP-generated probe signal amplitude on the probe-to-SMP protein concentration ratio is also consistent with such a redistribution process especially the tendency of the signal toward saturation at ratios above 7 nmol dye/mg protein, at which value a significant fraction of the probe membrane binding sites is apparently occupied; the transfer of additional probe to these sites would be expected to be energetically unfavorable because of charge repulsion between negatively charged probes in adjacent sites and because of the reduction in the system entropy as all sites approach occupancy.

The second-order rate law that the ATP-induced diBa-C_2-(5) spectral shift signal follows further suggests that the rate-limiting step for the probe response to $\Delta\Psi$ is the transfer of the probe from the bulk phase and/or the unstirred layer to SMP membrane binding sites, schematically described by:

free diBa-C_2-(5) + SMP binding site(s) + $\Delta\Psi \rightarrow\!\!\!\!\rightarrow$ complex

The absence of a slower phase in the probe time-resolved, ATP-dependent signal, however, suggests that the probe does not permeate the SMP membrane when $\Delta\Psi$ is present at least on a time scale of milliseconds to minutes. The invariance of all of the rate constants primarily characterizing the oxidation of cytochromes *c* and c_1 by ATP-driven reversed electron transport to the presence of diBa-C_2-(5) even at a high probe-to-membrane protein concentration ratio (Table I) is also consistent with the absence of an electrophoretically driven probe permeation of the membrane on a time scale of milliseconds to several minutes, since the permeation process is expected to compete with reversed electron transport for the energy from an ATP-generated $\Delta\Psi$ and hence to reduce the rate(s) at which reversed electron transport occurs. The reduction of the rate at which the ATP-dependent shift of the cytochrome-*c* oxidase soret band develops in pigeon heart mitochondria by the probe diS-C_3-(5) [21] is an example of the effect of probe permeation of the membrane on an energy-requiring process. A similar reduction in the rate at which the oxidase soret band shift develops by oxonol VI in SMP has also been observed [16].

The weak hydrophobicity of the ring ethyl groups together with the significant atomic charge essentially around the periphery of the probe especially that born by the oxygen and nitrogen ring moieties suggested by the molecular orbital calculations (see Fig. 1B) may render such a permeation process slow due to the high energy cost of moving the probe through the hydrophobic portion of the bilayer regardless of the probe orientation in the membrane bilayer even though the net charge that diBa-C_2-(5) bears is delocalized. In that a slower phase is lacking in the time-resolved potential-dependent signal in SMP, the behavior of

diBa-C_2-(5) is similar to that of merocyanine 540 (M540) that bears a localized charge on a sulfonate group, but differs from that of oxonol VI in SMP where a slower phase is observed and has been shown to be likely associated with membrane permeation by the latter probe as previously described [16].

The value of the second-order rate constant characterizing the ATP-induced diBa-C_2-(5) spectral shift signal, nominally $1 \cdot 10^7$ M^{-1} s^{-1}, is some two to three orders of magnitude higher than that of such rate constants, $1 \cdot 10^4$ M^{-1} s^{-1}, associated with the time course of merocyanine 540 [18] and oxonol VI [16], $3 \cdot 10^5$ M^{-1} s^{-1}, energy-dependent signals in the SMP preparation. The diBa-C_2-(5) rate constant value, however, is significantly lower than the limit expected for redistributing type potential-sensitive indicators. For the case in which the mechanism responsible for the probe response to $\Delta\Psi$ is the transfer of probe from the aqueous phase to binding sites on the membrane, the probe response time limit is expected to be that appropriate to a diffusion controlled bimolecular reaction. The general case of ligands approaching an impenetrable spherical surface with a large number of possible interaction sites has been discussed qualitatively by Berg [22] and treated quantitatively by Solc and Stockmayer [23] and more recently by Shoup et al. [24]; in these treatments the two reactants are modeled as spheres. In the limit of complete diffusion control with no steric or angular constraints on the reaction, the expression for the diffusion controlled rate constant, k_{DC}, simplifies to

$$k_{DC} = 4\pi DR \tag{4}$$

where D and R are, respectively, the sum of the translational diffusion coefficients and the effective radii of the two reactants. For the purpose of calculating k_{DC} characterizing the probe–SMP membrane interaction, the probe radius was taken to be one-half the length of the diBa-C_2-(5) molecule along the long axis, 7.9 Å; 250 Å was used as the SMP radius. The diffusion coefficients of both the probe and SMP were calculated from the Stokes-Einstein equations in the stick boundary limit, i.e., the limiting case in which the layer of medium immediately adjacent to the SMP and probe molecules moves at the same velocity as that of these two reacting species. The viscosity of a 0.25 M sucrose solution at 20 °C taken from the Handbook of Chemistry and Physics (CRC Press) was used in the calculation of the latter coefficients. The resulting order of magnitude value of k_{DC} was 10^{10} M^{-1} s^{-1}. This value of k_{DC} will, however, tend to be diminished by any steric constraints on the probe-SMP binding site interaction, charge repulsion effects, and site exclusion by the prior occupation of sites by passive SMP-probe binding, but the limiting value of k_{DC} does suggest that it may be possible to obtain rate constants in excess of the 10^7 M^{-1} s^{-1} value obtained from the data presented in Fig. 4 if these effects are minimized by appropriately designed potential-sensitive molecular probes. DiBa-C_2-(5) and similar barbituric acid derivatives thus appear to be promising as sources of fast-responding, redistributing type indicators of $\Delta\Psi$ in SMP preparations.

Acknowledgements

These investigations were supported in part by awards No. GM30552 from NIH and No. 2-4-01008 from the Department of Education. The diBa-C_2-(5) probe was generously provided by Professor A.S. Waggoner, Carnegie-Mellon University. The MACROMODEL molecular modeling package was furnished by Professor C. Still, Department of Chemistry, Columbia University. The authors have benefitted from discussions with Professor A.S. Allison regarding diffusion-controlled reactions and thank Ms. F. Tanious for assistance with the High Tech Ltd. stopped-flow apparatus and Ms. C. Bowden and Mr. D. Adams for assistance in generating the probe structure graphics.

References

1 Smith, J.C. (1990) Biochim. Biophys. Acta 1016, 1–28.
2 Bashford, C.L. (1981) Biosci. Rep. 1, 183–196.
3 Bashford, C.L. and Smith, J.C. (1979) Methods Enzymol. 55, 569–586.
4 Waggoner, A.S. (1979) J. Membr. Biol. 27, 317–334.
5 Waggoner, A.S. (1979) Annu. Rev. Biophys. Bioenerg. 8, 47–68.
6 Loew, L.M. (ed.) (1988) Spectroscopic Membrane Probes, CRC Press, Boca Raton.
7 Cohen, L.B. and Salzberg, B.M. (1978) Rev. Physiol. Biochem. Pharmacol. 83, 35–88.
8 DeWeer, P. and Salzberg, B.M. (eds.) (1986) Optical Methods in Cell Physiology, Vol. 40, Interscience-Wiley, New York.
9 DeGrooth, R. and Amesz, S. (1977) Biochim. Biophys. Acta 462, 247–258.
10 Dutton, P.L., Prince, R.C., Tiede, D.M., Petty, K.M., Kaufmann, K.J., Netzel, T.L., and Rentzepis, P.M. (1977) in Chlorophyll-Proteins, Reaction Centers, and Photosynthetic Membranes (Olson, J.M. and Hind, G., eds.), p. 213, Vol. 28, Brookhaven National Laboratory, Upton, New York.
11 Johnson, J.H., Lewis, A. and Gogel, G. (1981) Biochem. Biophys. Res. Commun. 103, 182–188.
12 Ehrenberg, B., Meiri, Z. and Loew, L.M. (1984) Photochem. Photobiol. 39, 199–205.
13 Thayer, W.S., Tu, Y.L. and Hinkle, P.C. (1977) J. Biol. Chem. 252, 8455–8458.
14 Bashford, C.L. and Smith, J.C. (1979) Biophys. J. 25, 81–85.
15 Lapin, L. (1975) Statistics Meaning and Method, pp. 360–361, Harcourt Brace Jovanovich, Inc., New York.
16 Smith, J.C. and Chance, B. (1979) J. Membr. Biol. 40, 255–282.
17 Chance, B. (1972) FEBS Lett. 23, 3–20.
18 Smith, J.C., Graves, J.M. and Williamson, M. (1984) Arch. Biochem. Biophys. 231, 430–453.
19 Mitchell, P. and Moyle, J. (1969) Eur. J. Biochem. 7, 471–484.

20 Bashford, C.L. and Thayer, W.S. (1977) J. Biol. Chem. 252, 8459–8463.
21 Bammel, B.P., Brand, J.A., Germon, W. and Smith, J.C. (1986) Arch. Biochem. Biophys. 244, 67–84.
22 Berg, H.C. (1983) Random Walks in Biology, pp. 30–34, Princeton University Press, Princeton.
23 Solc, K. and Stockmayer, W.H. (1971) J. Chem. Phys. 54, 2981–2988.
24 Shoup, D., Lipari, G., and Szabo, A. (1981) Biophys. J. 36, 697–714.